



Effect of PbS on ZnS nanostructure deposited using thermal evaporation: growth, morphological and structural study

B Muhammad Abdallah, M O Kakhia, A M Obied, and W A Zetoun

Department of Physics, Atomic Energy Commission of Syria, Damascus, Syria

E-mail: pscientific27@aec.org.sy

(Received 08 March 2021 ; in final form 11 May 2012)

Abstract

ZnS film has been deposited on PbS buffer layer using thermal evaporation, the ZnS film has nanostructure (nanowires) due to effect of PbS which play role of catalyst. This growth for non doped films have dense structure (for PbS and ZnS films). SEM morphology of ZnS/PbS, ZnS and PbS have been studied in details (surface and cross section). Atomic force microscopy (AFM) used to characterized the thins films (ZnS and PbS). X-ray photoelectron spectroscopy (XPS) and EDX techniques have utilized to know the chemical and stoichiometry of deposited films. The crystallographic properties have been studied using XRD patterns, it found that the results in Raman and XRD characterization have a good agreement. UV-Vis spectroscopy is used to acquire an idea about optical properties of thin films deposited on glass substrate. The deposited ZnS nanowires and thin film have hexagonal phase, which indicate to the buffer layer, which does not affects the structural but changes the growth mechanism. High Resolution Transmission Electron Microscope (HRTEM) images have confirmed the formation of ZnS nanowires..

Keywords: ZnS Nanowires, XRD and XPS characterization, SEM and HRTEM morphology

1. Introduction

The physical properties of semiconductors such as ZnS¹, ZnO^{2,3}, PbS⁴, SnO₂⁵ and SnS⁶ are greatly affected by the method of deposition film; with plasma like magnetron sputtering⁷ or without plasma such as thermal evaporation⁷, under vacuum or at atmosphere like spray pyrolysis⁸. Also, the compatibility of semiconducting with the substrate or the before layer⁹. The material nature¹⁰ (category)^{3, 11} and crystalline orientation of the substrate have distinguishing the nucleation processes (up to down or down to up nanotubes) and the growth mechanism dominated phases (cubic¹² or hexagonal⁸) of a thin film and its morphology as well as physical properties. Deposition of polycrystalline, single crystalline¹³ or amorphous thin films depends on the substrate as well as their chemistry (especially the interfaces) and growth conditions⁹. In the same deposition method, the used parameters (such as temperature and gas flux¹⁴), the stress and mismatch between the lattices of the substrate and the deposited material play a vital role on the properties of the deposited film, especially near the contact interface². Thickness of the films¹¹ can be decreased the effect of the lattice mismatch between the substrate and the films⁹.

PbS nanoparticles were used as a biosensors for the detection of bacterial samples¹⁵ as well as for pathogen monitoring¹⁶, and for its NLO (Nonlinear optical) properties of semiconductor application. Also, the variety of optical and electrical¹⁷ properties as well as applications of ZnS film attired the researchers groups to continues the development in laser technology, surface acoustic wave, diode¹⁸, Z- Scan and photoelectrical fields¹⁹.

The lattice mismatch is not always considered essential to influence on the growth mechanism and film quality, while the synthesizing method has curtail effect on film crystalline quality^{20, 21} and its behaviors, this phenomena has been observed and studied very well in previous works using several deposition techniques^{8, 12}. For very thin films the properties will be dominated by the several materials used in interface favorite the nanostructural nucleation and play a catalyst role⁷, which has been observed recently²². On the other hand, the optical, sensing and electrical⁷ properties have been sensible to the doped dose as well as metal nature like Cu, Zn, Pb or Ag⁵.

In this article, we have grown ZnS on PbS buffer layer as well as ZnS doped with PbS films on Si and

glass substrates, in order to investigate the morphology and structural properties of ZnS films as well as to control the mechanism of growth nanowires. Different techniques have been used to characterize the prepared ZnS films, such as X-ray diffraction (XRD), Dispersive X-ray Spectroscopy (EDX), photo-luminesces²³, UV-Vis, scanning electron microscope (SEM) and HRTEM. To our knowledge, this is first times to study the ZnS films with PbS as buffer layer (or seed layer) and comparing to the ZnS dope with PbS (12 wt %) using thermal evaporation method.

The thermal evaporation is simple and is interesting technique to obtain the good quality films (ZnS and PbS) as well as control their nanostructure.

2. Experimental

Three films were deposited using thermal evaporation method at 10^{-5} Torr pressure under different conditions; 1-ZnS /PbS film was deposited using two crucibles, the first for PbS powder and the second for ZnS powder, where the PbS deposited in the first and then we deposited ZnS film. 2- For thin PbS film, we used one crucible for deposited this film (PbS powder evaporated). 3- Finally, we used powders mixture 12 wt % PbS and 88 wt % ZnS in the same crucible.

SEM (TSCAN Vega\XMU) used to characterize the surface and growth morphology (surface view and cross section) and AFM used to show the morphology for ZnS/Si and PbS/Si thin films. Also, XPS and EDX have been utilized to obtain the composition of deposited films. XRD (Stoe Transmission X-ray diffractometer Stadi P) used to investigate the structural of the films (cubic or hexagonal phases). MicroRaman (Jobin-Yvon - LabRAM HR with He-Ne 633 nm laser) used to justify the vibrational modes in films²⁴, HRTEM used to observe the nanostructure growth for PbS:ZnS (PbS doped ZnS film). UV-Vis (Shimadzu UV-310PC Spectrophotometer) spectroscopy was used to obtain an idea about optical properties of deposited thin films on glass substrate cited in recent our works²⁴.

3. Results and discussions

3.1. SEM Study (Surface)

The films deposited on Si (100) substrate were characterized by SEM to reveal some information related to the thickness and the surface morphology. The film PbS/Si has nanosturctre (clasicaly growth with spherical form) as shown in figure (1-a), however, the ZnS/PbS film has nanowires growth due to deposited of PbS buffer layer as shown in figures (1-b), (1-c) and (1-d) where the magnifications were 10 k, 50 k and 100k, respectively.

The diameter of nanowires have less than 100 nm which is clearly in the figure (1-d) and the next paragraph, it will be discussed in details (SEM cross section). We have found in previous works, that the substrate (or buffer layer or seed layer) had a crucial role to favorite or disfavored the especial type of growth²⁵ as well as morphology using magnetron sputtering²⁶ or thermal evaporation¹ techniques. The ZnS nanowires is non dense structure while the PbS is thick and dense

structure.

3.2 AFM study for the surface

AFM characterization for thin films surface of PbS/Si and ZnS/Si are presented in figures (2-a) and (2-b), respectively. The morphology for both ZnS and PbS films are granular form. This classical growth has been conformed^{8, 12}, but to obtain nanowires/nanorods as well as nanostructures we need to catalyst for created and nucleated as shown in recent woks²⁷, where, we need to precursor and/or catalytic agent.

3.3. SEM study (Cross Section)

Cross section for ZnS thin films (this film deposited on Si using ZnS powder via thermal evaporation methods), SEM cross section of ZnS thin films (figure 3-a) show dense structure without nanowires form (classical growth), where it not used a catalyst for producing the growth mechanism. SEM cross section view was used to characterize growth morphology ZnS/PbS (where the ZnS film deposited on PbS thin film). The figure (3-b) shows nanosturtural (nanowires) in the top, whereas the PbS present dense film with the thickness of 300 nm). The diameter of nanowires has small and less 100 nm (figure 3-c and d), it confirms the PbS role as catalyst to create the nucleation of our seed layer to growth ZnS nanowires²⁸.

3.4 SEM and HRTEM study for PbS:ZnS

Figure (4-a) presents HRTEM images at bright field (BF) and similarly, figure (4-b) presents HRTEM at High-angle annular dark-field (HAADF) for PbS:ZnS nanowires film papered using 12 wt % PbS and 88 wt % ZnS (where the PbS as dopant for ZnS). HRTEM observation has shown that the structure of ZnS is nanowires with their diameter were variations from 10 nm to 50 nm. It looks like Nanowires and not Nanotubes structure.

Also, SEM cross section for PbS:ZnS film have shown that the nanowires growth with diameter less than 50 nm as seen in figure (5-a and 5-b) at 20 k and 50 k magnifications, respectively. The figure (5-c) and (5-d) present surface SEM images (top view) morphology for ZnS nanowires film, with small diameter and varied from 9 nm to 20 nm, where figure (4-c) SEM images at 100 k and figure (4-d) at 200 k magnification. So SEM images (surface and cross section) have confirmed the creation of nanowires PbS:ZnS film.

3.5 XRD Study

Figure (6) shows XRD pattern of PbS films deposited on Si(100), all reflected peaks correspond to the cubic structure of PbS with lattice parameters $a = 0.59143$ nm. All peaks (111) at 26.10° , (200) at 30.15° and (220) at 43.22° , are in good agreement with the database (PDF number 78-1054). The peak (002) at 28.55° for corresponds to ZnS wurtzite (hexagonal) phase in ZnS/PbS nanowires. This results accorded with recent study, where we obtained ZnS hexagonal structural using spray pyrolysis⁸. But in previous work¹², it was found that the ZnS polycrystalline as cubic structural using

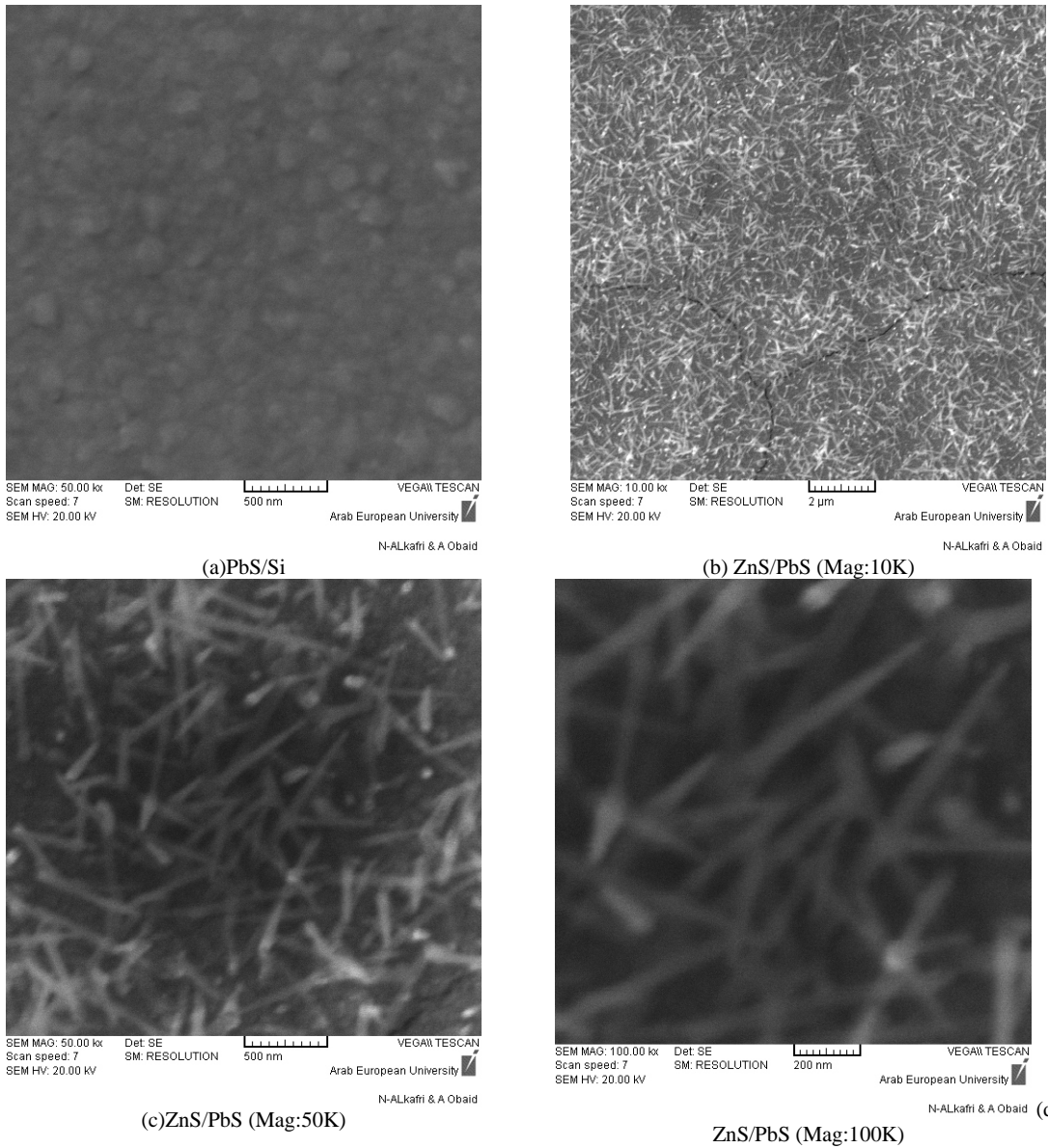


Figure. 1 SEM images for (a) PbS thin film, and SEM images for ZnS/PbS nanowires at (b) 10 k magnification, (c) at 50 k magnification and (d) at 100k magnification.

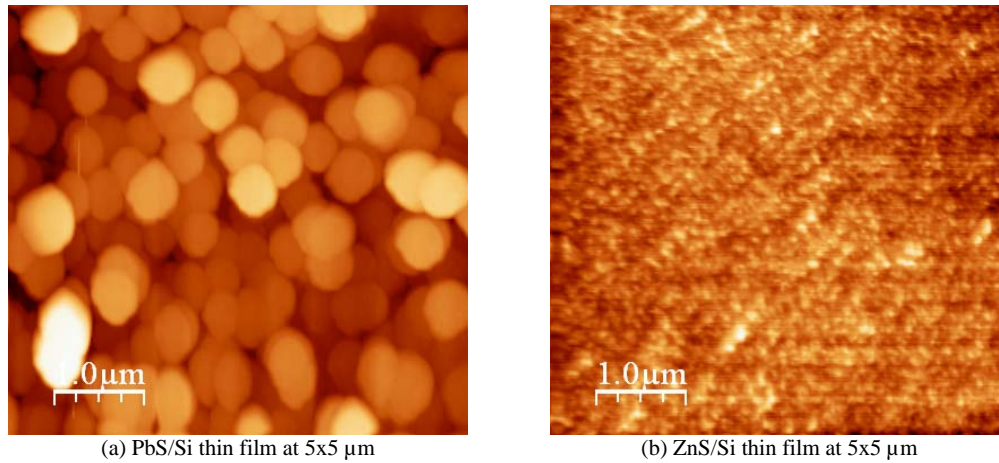


Figure. 2 AFM images for (a) PbS/Si thin film and (b) for ZnS/Si thin film at 5x5 μm.

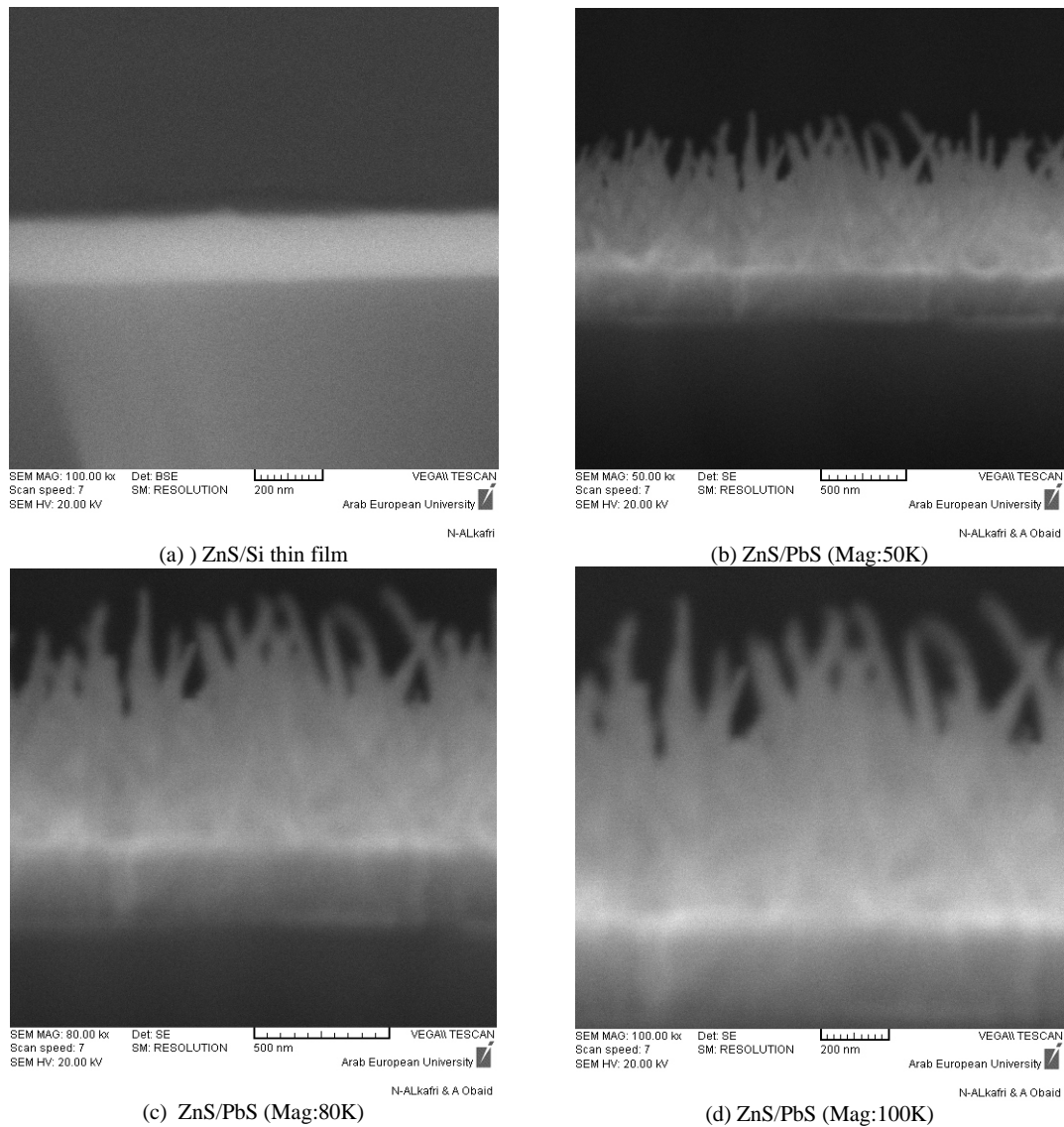
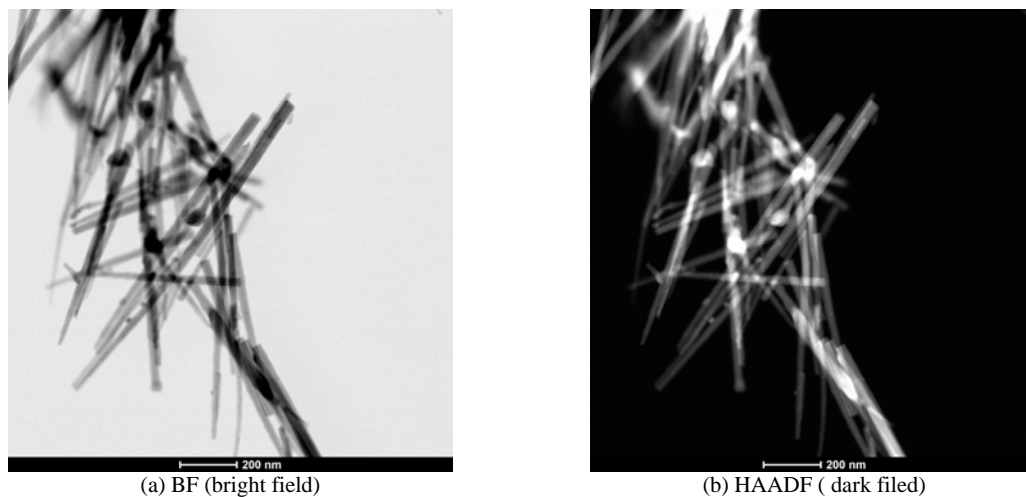


Figure. 3 SEM cross sections images (a) for ZnS thin film and for ZnS/PbS nanowires (b) at 50 k magnification, (c) at 80 k magnification and (d) at 100 k magnification.



Figures. 4 HRTEM images (a) BF (bright field) and (b) HAADF (dark filed) mode.

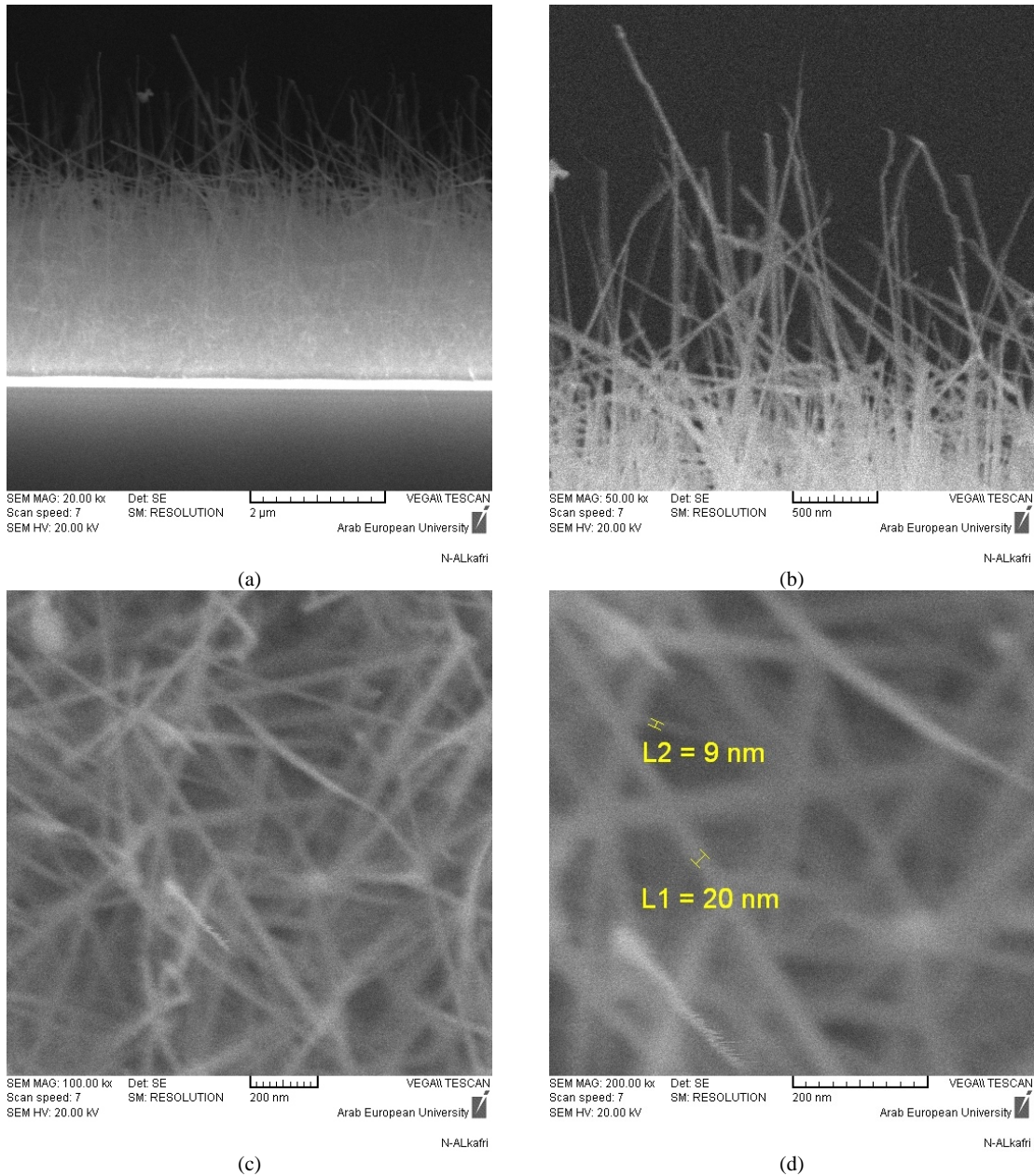


Figure. 5 (a) and (b) SEM cross section images at 20 K and 50 K magnifications, respectively. (c) and (d) SEM images for surface at 100 k and 200 k magnifications, respectively.

electron gun deposition. The XRD pattern for PbS:ZnS nanowires (12 wt % PbS) has also wurtzite with (002) as preferential orientation, with two peak at 26.86° and 30.53° corresponding to (100) and (101) orientation, respectively. The peak at 31.33° is due to cubic Pb according with the PDF Number : 4-686 due to disassociated the powder of PbS in heating behind the evaporation process where the crucible contain ZnS and PbS powder.

3.6 UV-Vis Study

UV-Vis transmittance spectra show the transparency of two films (PbS film and ZnS/PbS film) the small value of transmittance of PbS properties is low transparency in UV domain (which it has high transparency in IR

domain) (figure 7-a). The optical transmittance provides useful information about the optical band gap of the semiconductor²⁹. The optical band gap was calculated from UV-Vis spectra using Tauc formula, and it is about 1.61 eV for PbS thin film only (figure 7-b).

Also, the figure (7-c) shows the band gap is about 1.62 eV for PbS layer in film ZnS/PbS nanowires. The situated band gap at 2.27 eV is due to PbS doped ZnS (or the PbS incorporated or quantum dot PbS in ZnS nanowires); As the particle size decreases, the band gap of semiconductor is found to increase; this is known as the quantum size effect⁴.

3.7 Raman Study

He-Ne laser (633 nm) has been used to examine the

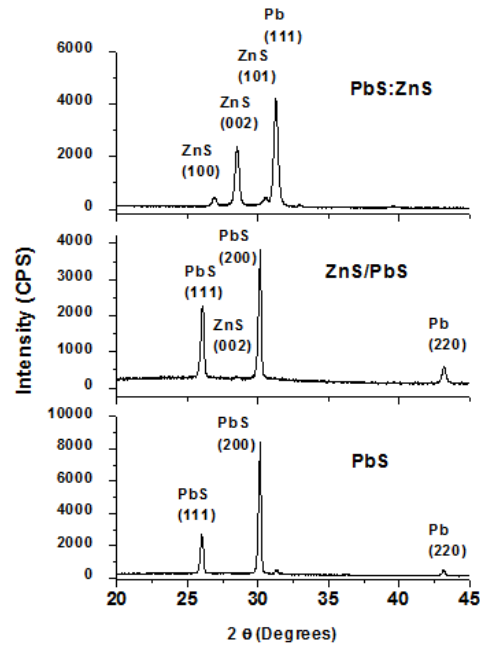


Figure.6 XRD pattern for PbS thin film, ZnS/PbS nanowires and for PbS:ZnS nanowires deposited on Si (100) substrate.

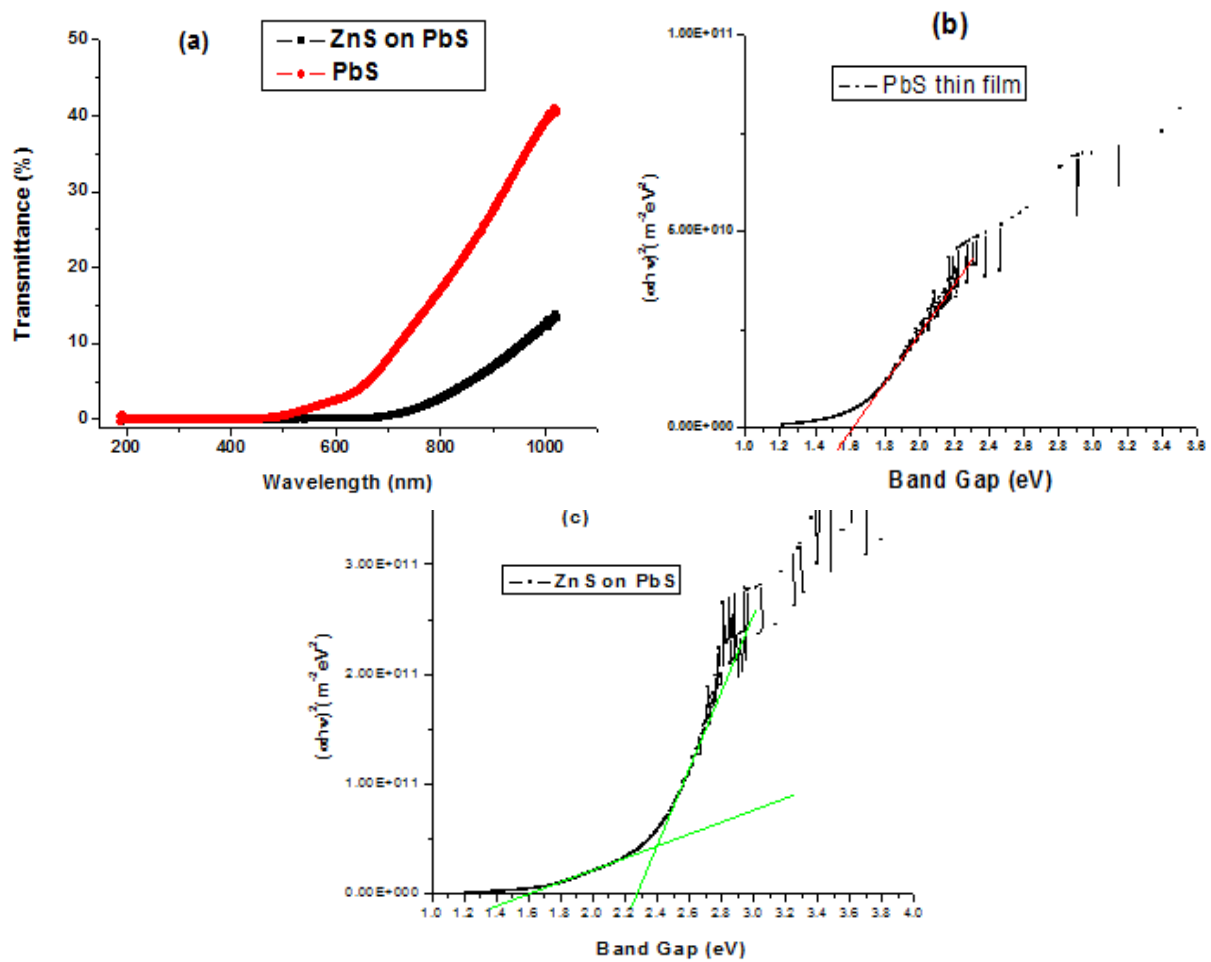


Figure. 7 (a) UV-Vis spectra for PbS (red color) film and ZnS/PbS nanowires (black color) and their corresponding band gap (b) for PbS thin film and (c) ZnS/PbS nanowires deposited on glass substrates.

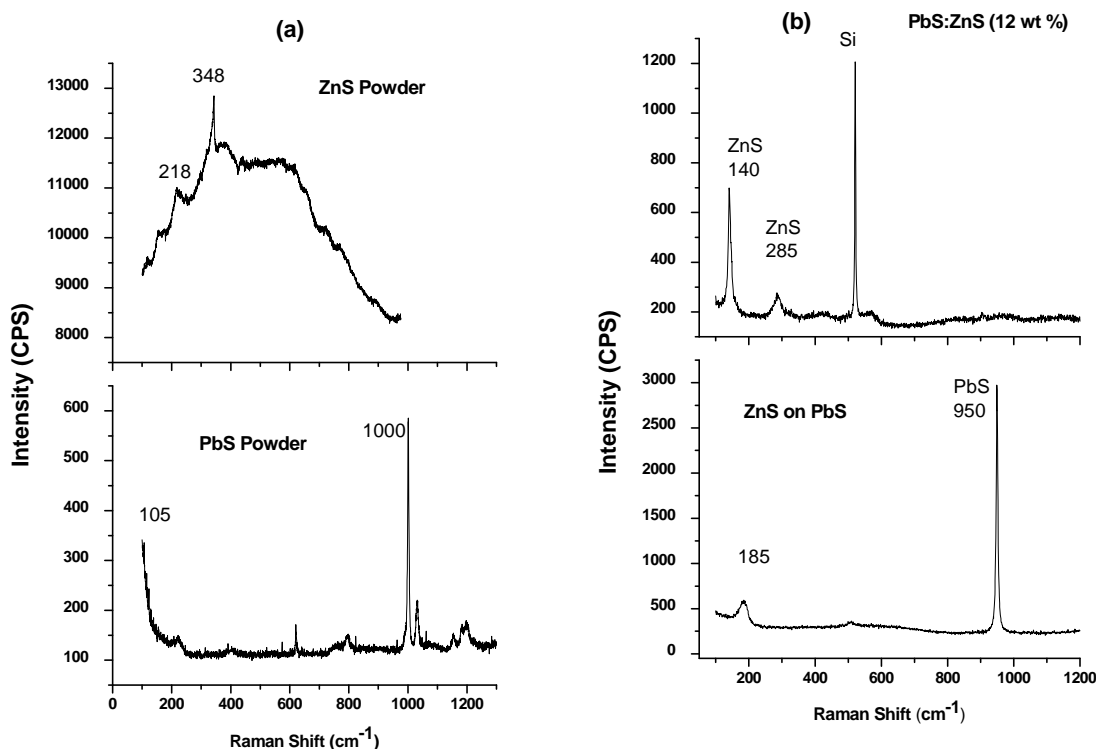


Figure. 8 Raman spectra(a) of PbS and ZnS powders and (b) for PbS thin film and ZnS/PbS nanowires.

Raman vibrational modes of PbS and ZnS powders which has shown in figure (8-a). Raman spectrum peaks at 105 cm^{-1} and 1000 cm^{-1} for PbS powder might be attributed to a combination of longitudinal and transverse acoustic (LA + TA) phonon modes and is due to the anglesite PbSO_4 Phase⁴. Similarly, Raman spectra for ZnS powder have shown dominated peak at 348 cm^{-1} by the longitudinal optical phonon³⁰ and large peak at 218 cm^{-1} correspond longitudinal acoustic phonon for ZnS¹.

The peaks at 185 cm^{-1} could be due to PbSO or longitudinal optical (LO) phonons for PbS³¹ and the intense peak at 950 cm^{-1} is due to PbS for ZnS film on PbS as shown in figure (8-b). Also, PbS:ZnS film nanowires (12 PbS wt % and 88 PbS wt %) present two peaks at 140 cm^{-1} and 285 cm^{-1} the transverse optical phonon peak around 140 cm^{-1} (TO -2LA) related for ZnS³² and the transverse optical phonon peak around 285 cm^{-1} associated to ZnS, respectively.

3.8 EDX and XPS Study

EDX technique was used for (figure 9-a) PbS/Si thin film and (figure 9-b) for ZnS/PbS/Si nanowires to observe the elements composition of the films. We have found Pb and S elements are mainly components of this studied film and O is found in small quantity, which, it considered as contamination. Table 1 presents the element percentage of Pb and S and the ratio was about 1 which confirms that the film is stoichiometry. The EDX spectra for ZnS/PbS/Si show Zn, Pb and S peaks with important quantity (because we have two films or two

layer, ZnS nanowires in the top and PbS in the bottom) so the S elements is coexisted in two layers, and consequently the EDX spectrum just for evidence to presence these elements.

For further investigation of the chemical composition of the product, XPS scan of the sample was performed (figure 10 (a) and (b)). In order to compensate the surface charging effect C1s signal (284 eV) has used as a reference signal. XPS curves were fitted after adjusting to the theoretical curves. Detailed spectra for the PbS/Si thin film show Pb_{4f} , S_{2p} , C_{1s} and O_{1s} regions and related data are presented in figure (10-a). However, XPS curve for ZnS/Si thin film (without PbS buffer layer) show Zn_{2p} , S_{2p} , C_{1s} and O_{1s} regions, The results of XPS surface analyses are summarized in table 2, which confirm the formation of PbS (in figure 10-a) and ZnS (in figure 10-b) compound and they are quite stoichiometry of the films. Moreover, there was a strong indication of the presence of traces of, ZnO, PbO, CO and PbSO_3 on the surface of the films due to preparation and measurement conditions. The ZnS nanowires film on PbS (ZnS /PbS) in figure (10-c) expedited Zn_{2p} , S_{2p} , C_{1s} , O_{1s} and Pb_{4f} , where the presence of the peak of elements Pb_{4f} in the XPS spectra (table 2) indicates that the Pb in the nanowires does not poisoning or booked up in the interface (bottom in the nanowires), but it is thawed in the nanowires.

XPS confirms the presence the Pb and S for PbS thin film, also as well as the presence of Zn and S elements for ZnS thin films. Also, presence of the important quantity for O and C in the surface is due to humidity

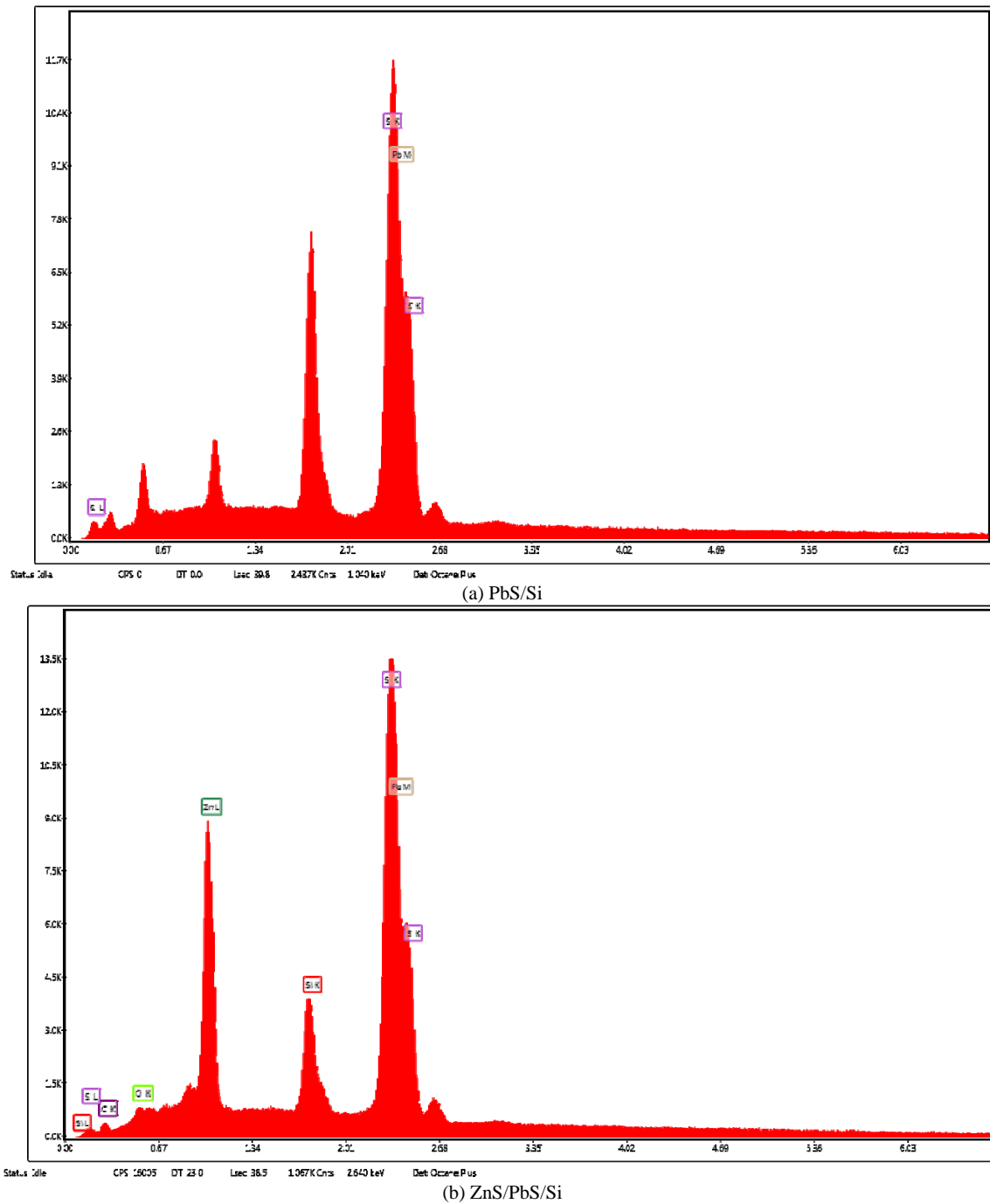


Figure. 9 EDX spectra for (a) PbS/Si thin film and (b) for ZnS/PbS/Si nanowires.

absorbed in the two thin films as considerate that the XPS techniques analyze just the superficial layer (depth varied between 5 to 10 nm as maxima). The EDX and XPS confirmed stoichiometry of deposited films with low contamination of oxygen which present that the thermal evaporation is interesting technique to obtain the good quality ZnS and PbS films as well as control their nanostructure.

4 Conclusion

ZnS film deposited on PbS buffer layer has compared with ZnS/Si and PbS/Si using thermal evaporation. The ZnS on PbS has nanowires structure, PbS buffer layer playing role of catalyst. This growth for PbS and ZnS thin films typically has dense structure. SEM and AFM morphology show that the PbS and ZnS separated films have granular form, while growth ZnS/PbS has nanowires. XPS and EDX utilized to know the elements

Table. 1 Atomic percentage for PbS/Si film using EDX

Element	Weight %	Atomic %
S _K	15.64	54.5
Pb _M	84.36	45.5

Table. 2 Atomic percentage for O, C, S and Zn elements from XPS analysis for PbS thin ZnS film and ZnS nanowires on PbS

At %	Pb _{4F}	S _{2P}	O _{1S}	C _{1S}	Zn
position	138	161	531	284	1020
PbS/Si thin film	5.85	8.90	25.43	50.82	
ZnS/Si thin film	-	2.46	36.86	52.36	2.46
PbS:ZnS nanowires	1.46	33.36	16.39	43.69	5.10

composition and stoichiometry of deposited films. The crystallographic properties have been studied using XRD patterns and Raman, The ZnS nanowires and thin film have hexagonal phase, which indicate to the buffer layer not affects the structural but change the growth mechanism. Optical characterizations have been effected using UV-Vis spectroscopy to obtain the transparency as well as the optical band gap. SEM and HRTEM techniques confirm the creation the nanowires where we use the PbS as dopant for ZnS film in our condition.

References

1. B Abdallah, M Kakhia, and N Alkafri Investigation of zns nanotubes films: Morphological, structural and optical properties. *Journal of Nano Research*. **60** (2019) 142.
2. S Al-Khawaja, B Abdallah, S Abou Shaker, and M Kakhia, Thickness effect on stress, structural, electrical and sensing properties of (002) preferentially oriented undoped zno thin films. *Composite Interfaces*. **22** (3) (2015) 221.
3. A S Vishnoi, R Kumar, and A Singh BP, Effect of substrate on physical properties of pulse laser deposited zno thin films. *Journal of Intense Pulsed Lasers and Applications in Advanced Physics*. **4** (1) (2014).
4. B Abdallah, K Mahmoud, and Z Walaa, Alkafri MN. Synthesizing of zns and zno nanotubes films deposited by thermal evaporation: Morphological, structural and optical properties. *Materials Research Express*. (2019).
5. B Abdallah, AK Jazmati, and M Kakhia, Physical, optical and sensing properties of sprayed zinc doped tin oxide films. *Optik*. **158** (2018) 1113.
6. A Basak, A Hati, and A Mondal, Singh UP, Taheruddin SK. Effect of substrate on the structural, optical and electrical properties of sns thin films grown by thermal evaporation method. *Thin Solid Films*. **645** (2018) 97.
7. AK Jazmati, B Abdallah, and F Lahlah, and S Abou Shaker, Photoluminescence and optical response of zno films deposited on silicon and glass substrates. *Materials Research Express*. **6** (8) (2019) 086401.
8. K Alnama, B Abdallah, and S Kanaan, Deposition of zns thin film by ultrasonic spray pyrolysis: Effect of thickness on the crystallographic and electrical properties. *Composite Interfaces*. **24** (5) (2017) 499.
9. S Rahmane, B Abdallah, A Soussou, E Gautron, P-Y Jouan, L Le Brizoual, N Barreau, A Soltani, and MA Djouadi. Epitaxial growth of zno thin films on aln substrates deposited at low temperature by magnetron sputtering. *physica status solidi (a)*. **207** (7) (2010) 1604.
10. B Abdallah and MS Rihawy, Ion beam measurements for the investigation of tin thin films deposited on different substrates by vacuum arc discharge. *Nuclear Instruments and Methods in Physics Research Section B: Beam Interactions with Materials and Atoms*. **441** (2019) 33.
11. B Abdallah, C Duquenne, MP Besland, E Gautron, PY Jouan, PY Tessier, J Brault, Y Cordier, and MA Djouadi, Thickness and substrate effects on aln thin film growth at room temperature. *Eur Phys J Appl Phys*. **43** (3) (2008) 309.
12. B Abdallah, K Alnama, and F Nasrallah, Deposition of zns thin films by electron beam evaporation technique, effect of thickness on the crystallographic and optical properties. *Modern Physics Letters B*. **33** (04) (2019) 1950034.
13. AK Jazmati and B Abdallah, Optical and structural study of zno thin films deposited by rf magnetron sputtering at different thicknesses: A comparison with single crystal. *Materials Research* (2018).
14. B Abdallah, AK Jazmati, and R Refaai, Oxygen effect on structural and optical properties of zno thin films deposited by rf magnetron sputtering. *Materials Research*. **20** (3) (2017) 607.
15. D Himadri, D Pranayee, SK Kumar. Synthesis of pbs nanoparticles and its potential as a biosensor based on memristic properties. *Journal of Nanoscience and Technology*. **4** (5) (2018) 500.
16. PJ Vikesland and KR Wigginton, Nanomaterial enabled biosensors for pathogen monitoring- a review. *Environmental Science & Technology*. **44**

- (10) (2010) 3656.
17. K Alnama, B Abdallah, and S Kanaan. Deposition of zns thin film by ultrasonic spray pyrolysis: Effect of thickness on the crystallographic and electrical properties. *Composite Interfaces*. **24** (5) (2016) 499.
 18. F Kurnia, Ng YH, Y Tang, R Amal, N Valanoor, JN Hart, Zns thin films for visible-light active photoelectrodes: Effect of film morphology and crystal structure. *Crystal Growth & Design*. **16** (5) (2016) 2461.
 19. B Abdallah, MD Zidan, and A Allahham, Deposition zns films by rf magnetron sputtering: Structural and optical properties sing z-scan technique. *dend to Journal* (2019).
 20. D Mendil, F Challali, T Touam, A Chelouche, AH Souici, S Ouhenia, and D Djouadi, Influence of growth time and substrate type on the microstructure and luminescence properties of zno thin films deposited by rf sputtering. *Journal of Luminescence*. **215** (2019) 116631.
 21. AK Jazmati, B Abdallah, Optical and structural study of zno thin films deposited by rf magnetron sputtering at different thicknesses: A comparison with single crystal. *Materials Research*. **21** (2018).
 22. P Hazra, SK Singh, and S Jit, Impact of surface morphology of si substrate on performance of si/zno heterojunction devices grown by atomic layer deposition technique. *Journal of Vacuum Science & Technology A: Vacuum, Surfaces, and Films*. **33** (1) (2014) 01A114.
 23. Fu YQ, L Garcia-Gancedo, HF Pang, S Porro, YW Gu, J K Luo XTZ, F Placido, JIB Wilson, AJ Flewitt, W I Milne, Microfluidics based on zno/nanocrystalline diamond surface acoustic wave devices. *Biomicrofluidics*. **6** (024105) (2012). 024101.
 24. B Abdallah, M Kakhia, Zetoune, and W Structural, optical and sensing properties of zns thick films deposited by rf magnetron sputtering technique at different powers. *World Journal of Engineering*. **17** (3) (2020) 381.
 25. S Rahmane, B Abdallah, A Soussou, E Gautron, PY Jouan, L Le Brizoual, N Barreau, A Soltani, MA Djouadi, Epitaxial growth of zno thin films on aln substrates deposited at low temperature by magnetron sputtering. *Physica Status Solidi (a)*. **207** (7) (2010) 1604.
 26. C Duquenne, MA Djouadi, PY Tessier, PY Jouan, MP Besland, C Brylinski, R Aubry, S Delage, Epitaxial growth of aluminum nitride on algan by reactive sputtering at low temperature. *Applied Physics Letters*. **93** (5) (2008) 052905.
 27. B Abadllah, B Assfour, M Kakhia, and A Bumajdad. Hrtem, xps and xrd characterization of zns/pbs nanorods prepared by thermal evaporation technique. *Nanosystems: Physics, Chemistry, Mathematics*. **11** (5) (2020) 1.
 28. J Alyones, M Salameh, and B Abdallah, Investigation of pressure effect on structural, mechanical properties and corrosion performance of crn thin films. *Silicon* (2019).
 29. B Abdallah, and S Al-Khawaja, Optical and electrical characterization of (002) preferentially oriented n-zno/p-si heterostructure. *Acta Physica Polonica* **128** (2015) 283.
 30. GT Mazitova, KI Kienskaya, DA Ivanova, IA Belova, IA Butorova, MV Sardushkin, Synthesis and properties of zinc oxide nanoparticles: Advances and prospects. *Review Journal of Chemistry*. **9** (2) (2019) 127.
 31. TS Shyju, S Anandhi, R Sivakumar, R Gopalakrishnan, Studies on lead sulfide (pbs) semiconducting thin films deposited from nanoparticles and its nlo application. *International Journal of Nanoscience*. **13** (01) (2014) 1450001.
 32. J Serrano, AH Romero, FJ Manjón, R Lauck, M Cardona, and A Rubio, Pressure dependence of the lattice dynamics of zno: An ab initio approach. *Physical Review B*. **69** (9) (2004) 094306.